S1.1 BET surface area and pore size

As shown in Table S1, most of the prepared HTlcs have high surface area (greater than 100 $m^2\ g^{-1}$), the only exception being Cu-Al HTlcs (59 $m^2\ g^{-1}$).

Fig. S3 shows the nitrogen physisorption isotherms and BJH pore size distributions for the HTlcs, $M^{2+}(M^{3+})O$ and MO materials. The isotherms of HTlcs and most of the $M^{2+}(M^{3+})O$ systems has the characteristic type IV shape indicating that they are mesoporous materials. Compared to the $M^{2+}(M^{3+})O$ systems, the pore size distributions of the HTlcs were narrower and the pore diameters were smaller. The BJH pore diameters and pore volumes confirmed that Cu(Fe)O was an non-porous material, which explained its low surface area. The BJH pore diameters and pore volumes also illustrated that most of the prepared MO were non-porous materials.

S1.2 The basic strengths and basicity of the catalysts

CO_2 TPD measurements were performed to assess the base site strength and concentration. Fig.S4 shows the rate of CO_2 desorption, normalized to the sample loading, as a function of temperature for each $M^{2+}(M^{3+})O$ support and $KF/M^{2+}(M^{3+})O$-cn catalyst. The desorption profiles for the $M^{2+}(M^{3+})O$ supports showed one apparent desorption peak with a maximum at 100 °C.

For all the $KF/M^{2+}(M^{3+})O$-cn samples, with the exception of KF/Co(Cr)O-cn, only a single apparent desorption feature with a maximum 100 °C was observed. Above 100 °C, there were no desorption peaks for $KF/M^{2+}(M^{3+})O$-cn. The desorption profiles for $KF/M^{2+}(M^{3+})O$-cn were similar to the corresponding supports, falsely implying that KF doping did not increase the basic strength of prepared $KF/M^{2+}(M^{3+})O$-cn catalysts. However, both the Hammett indicators measurements are consistent with increase in base strength upon KF doping. This apparent anomaly could arise from the high basic strength of KF/M^{2+}(M^{3+})O-cn resulting in CO_2 being so strongly adsorbed on its surface that it is not desorbed below 500 °C. This suggestion is consistent with the structure analysis in section 3.2. which showed that KOH was formed on the surface of KF/M^{2+}(M^{3+})O-cn catalysts (Eq. (1)-(5)). The KOH formed would be expected to chemisorb CO_2 very strongly.

KF/Co(Cr)O-cn did not show a desorption peak at about 100 °C, illustrating that the number of base sites may be lower than that of the support alone. The reason for this may be similar to that for KF/Cr_2O_3-cn (Eq. (6)).

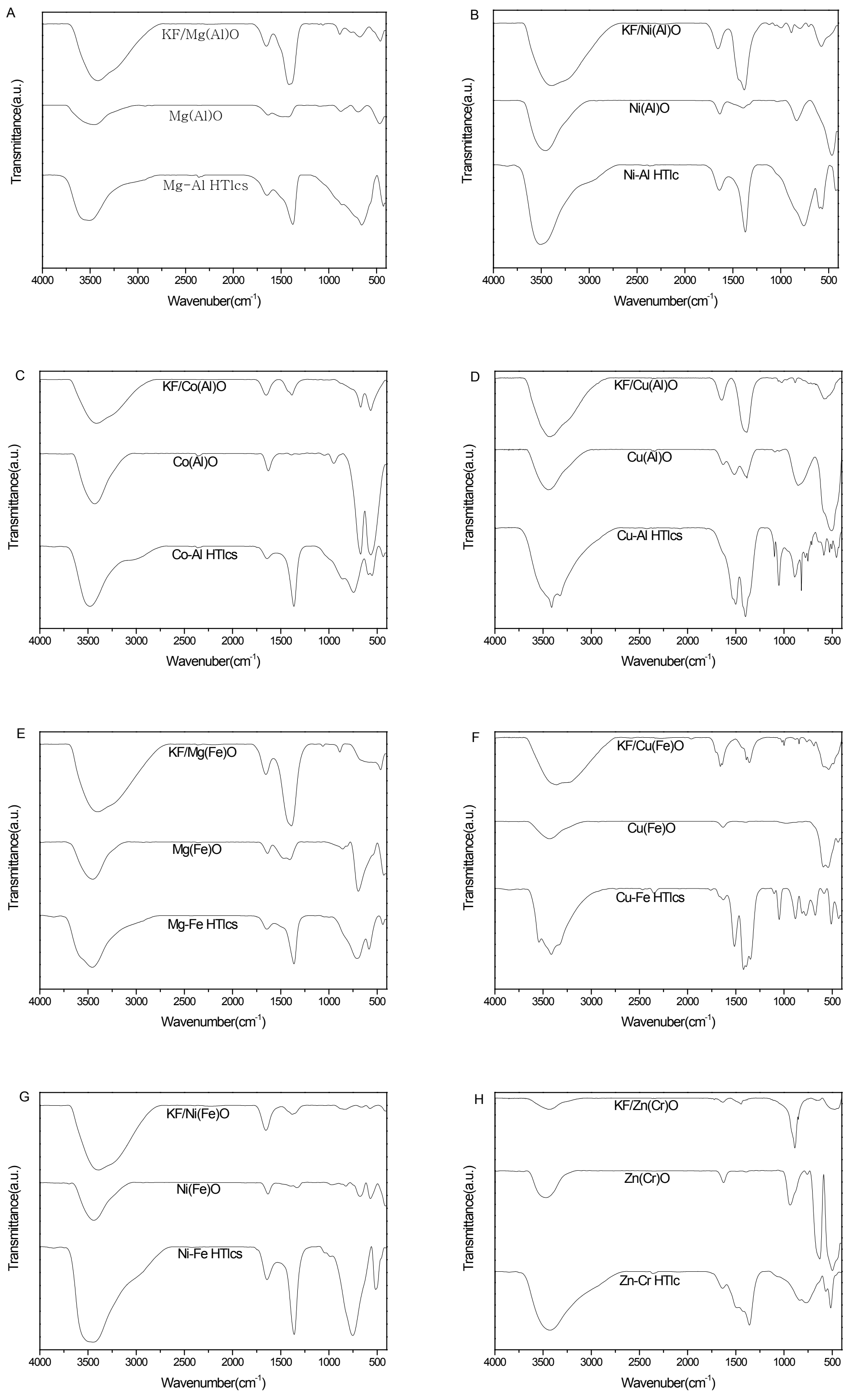
A
KF/Mg(Al)O
Mg(Al)O
Mg-Al HTlcs
B
KF/Ni(Al)O
Ni(Al)O
Ni-Al HTlc
C
KF/Co(Al)O
Co(Al)O
Co-Al HTlcs
D
KF/Cu(Al)O
Cu(Al)O
Cu-Al HTlcs
E
KF/Mg(Fe)O
Mg(Fe)O
Mg-Fe HTlcs
F
KF/Cu(Fe)O
Cu(Fe)O
Cu-Fe HTlcs
G
KF/Ni(Fe)O
Ni(Fe)O
Ni-Fe HTlcs
H
KF/Zn(Cr)O
Zn(Cr)O
Zn-Cr HTlc
Transmittance(a.u.)
4000 3500 3000 2500 2000 1500 1000 500
Wavenuber(cm-1)
Wavenumber(cm-1)

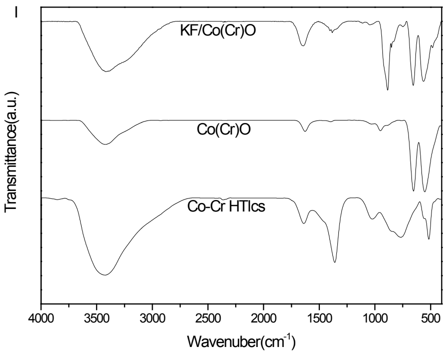

Fig. S1 FTIR spectra of HTlcs, $M^{2+}(M^{3+})O$ and KF/$M^{2+}(M^{3+})O$-cn.

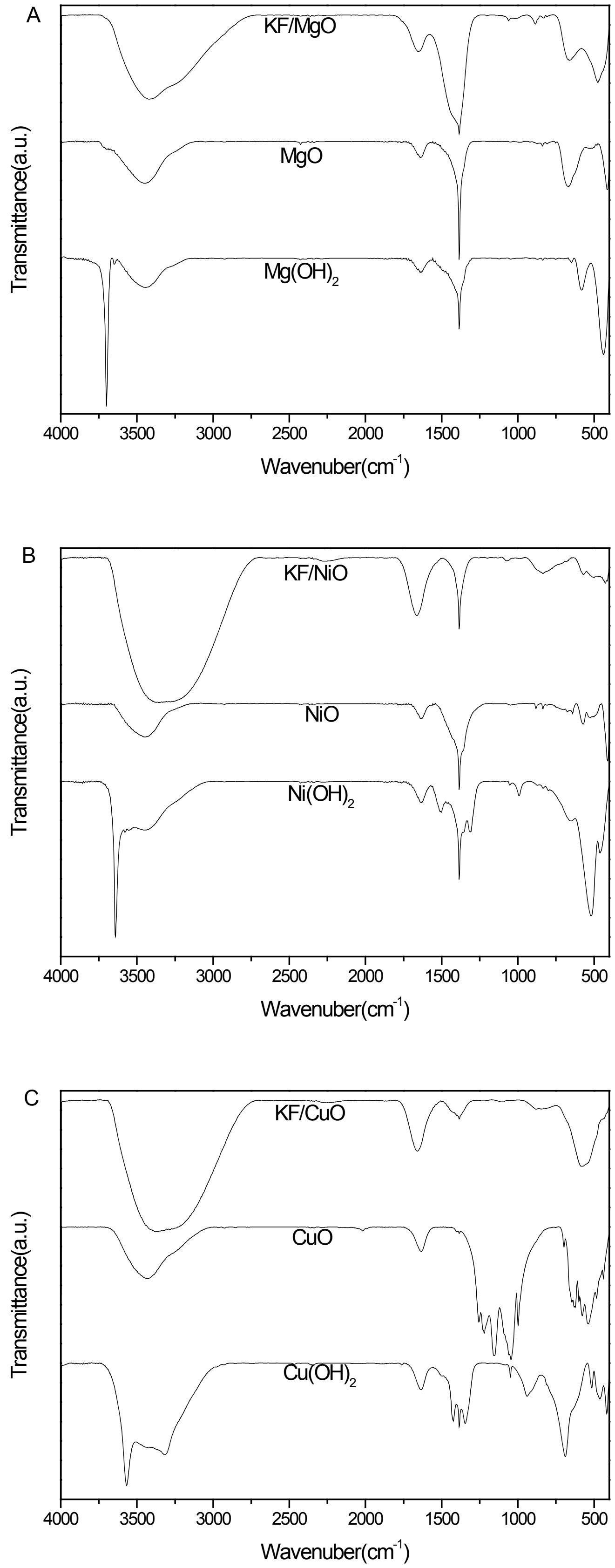

Fig. S2 FTIR spectra of $M(OH)_2$, MO and KF/MO-cn.

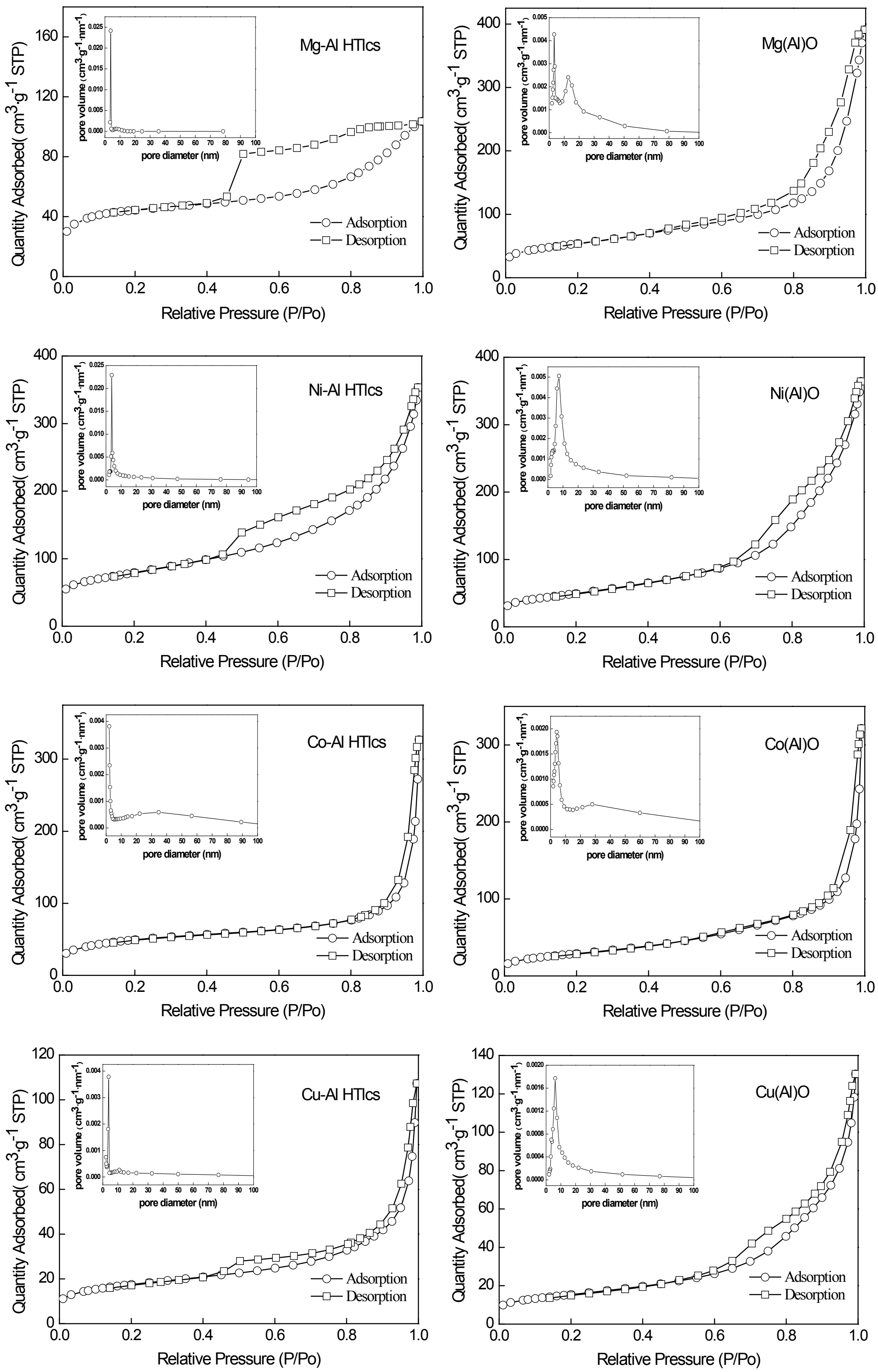

Fig.S3-continued

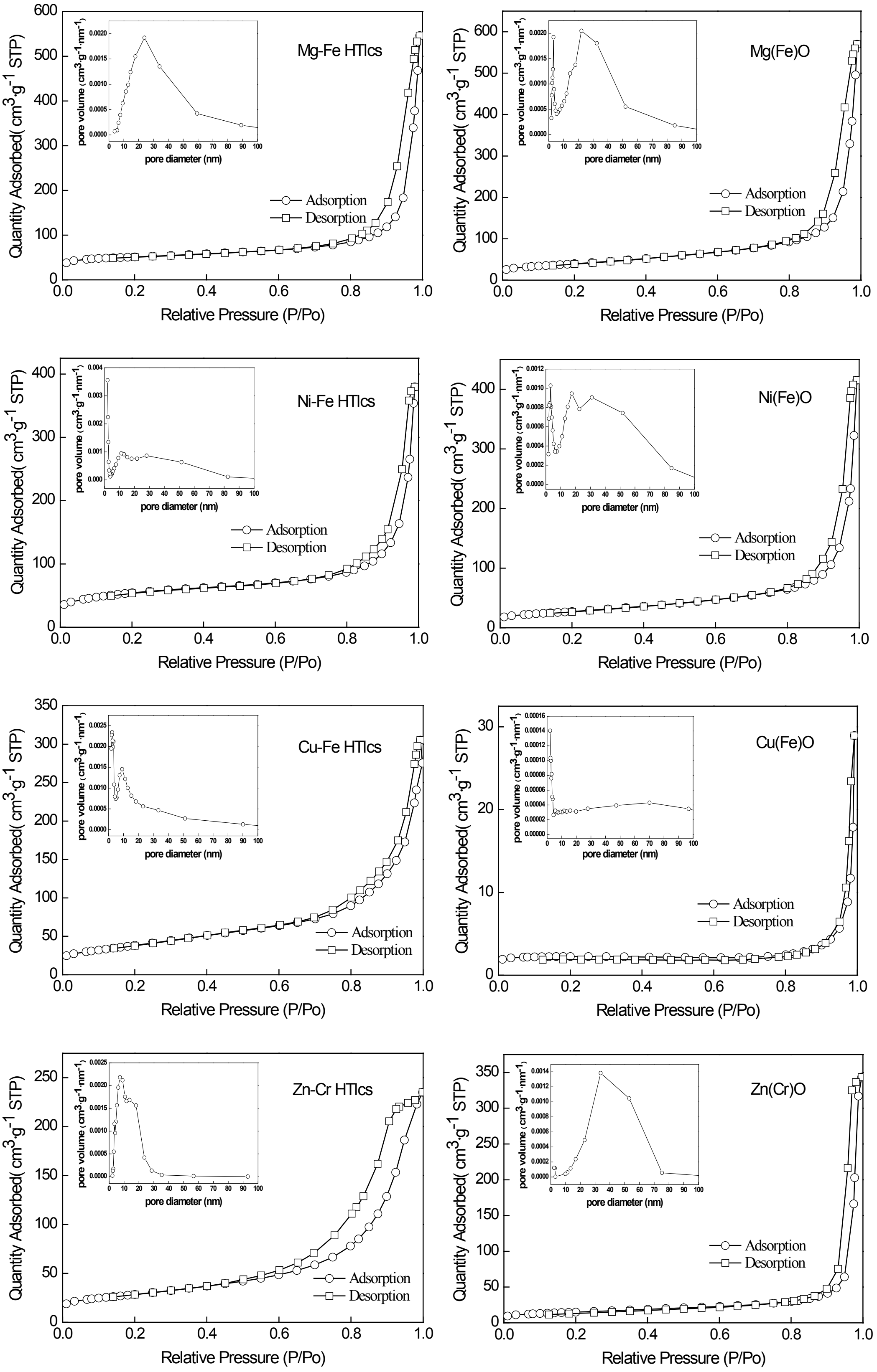

Fig.S3-continued

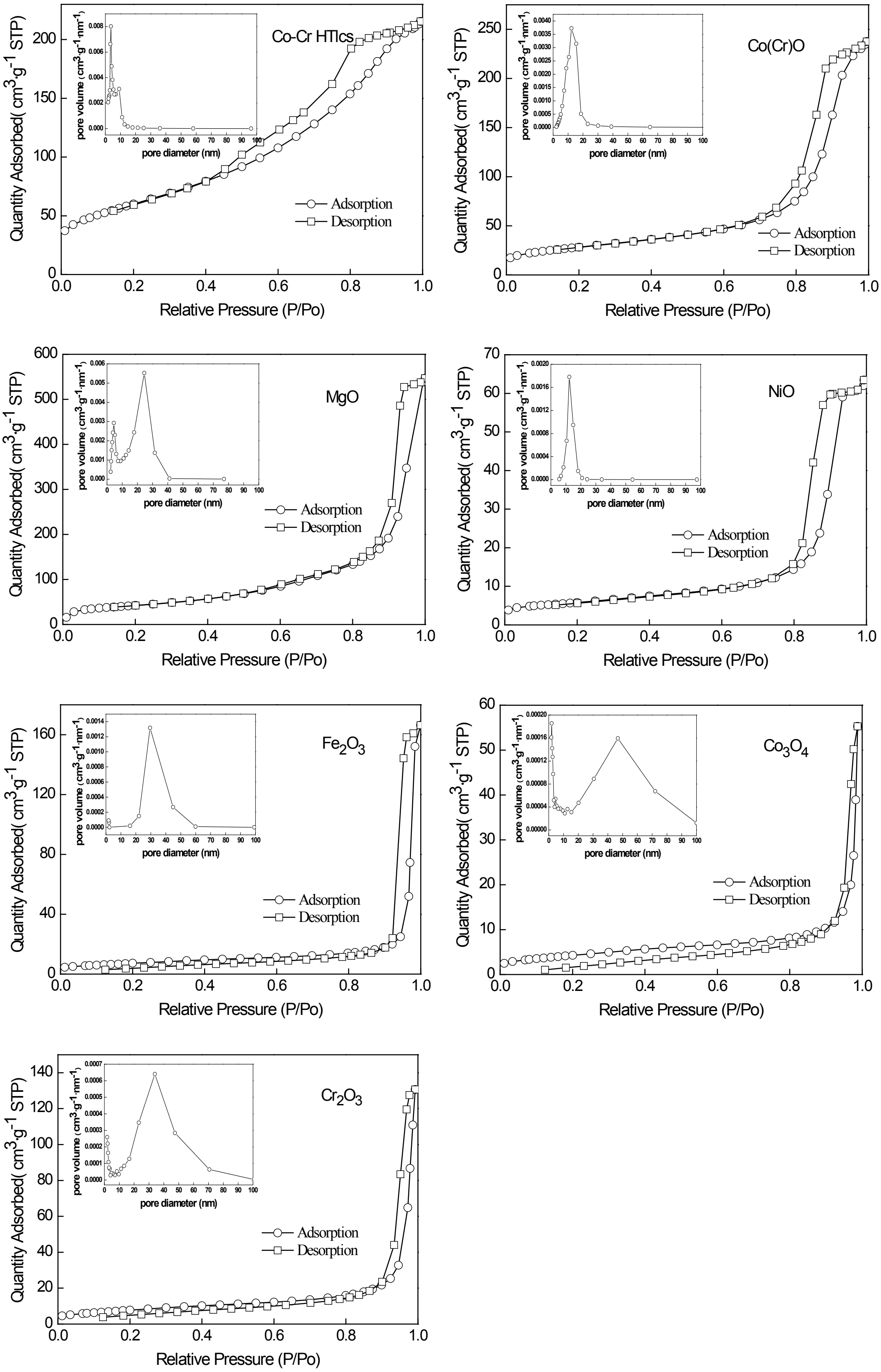

Fig. S3 **Physisorption isotherms and BJH pore size distribution for HTlcs, $M^{2+}(M^{3+})O$ and MO.**

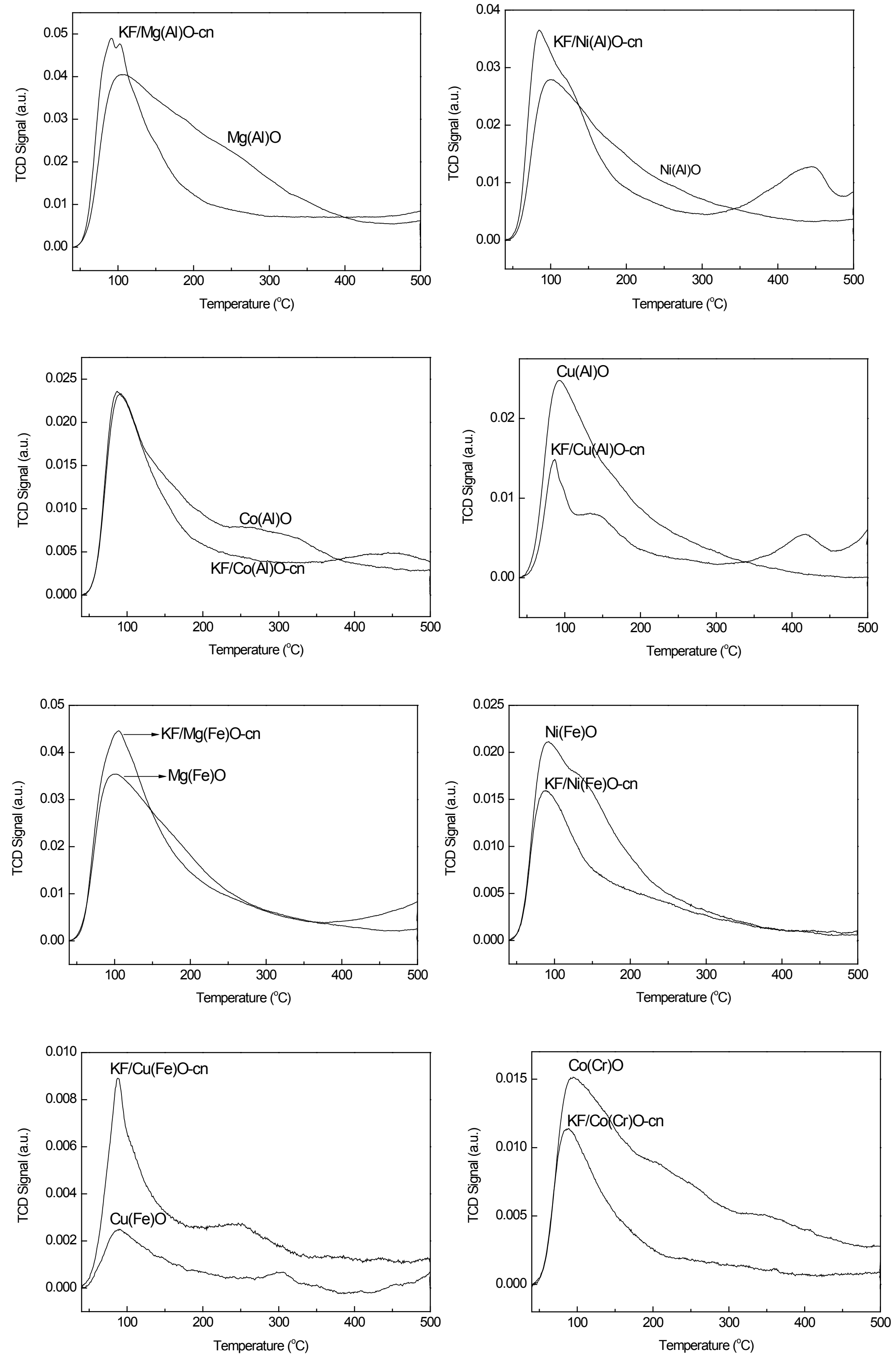
KF/Mg(Al)O-cn
Mg(Al)O
KF/Ni(Al)O-cn
Ni(Al)O
Co(Al)O
KF/Co(Al)O-cn
Cu(Al)O
KF/Cu(Al)O-cn
KF/Mg(Fe)O-cn
Mg(Fe)O
Ni(Fe)O
KF/Ni(Fe)O-cn
KF/Cu(Fe)O-cn
Cu(Fe)O
Co(Cr)O
KF/Co(Cr)O-cn
TCD Signal (a.u.)
Temperature (°C)

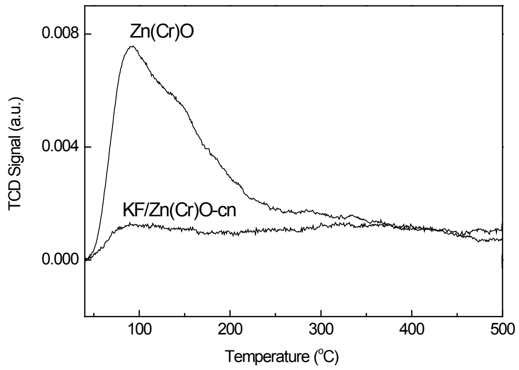

Fig.S4 TPD profiles of CO_2 adsorbed on $M^{2+}(M^{3+})O$ and $KF/M^{2+}(M^{3+})O$-cn materials.

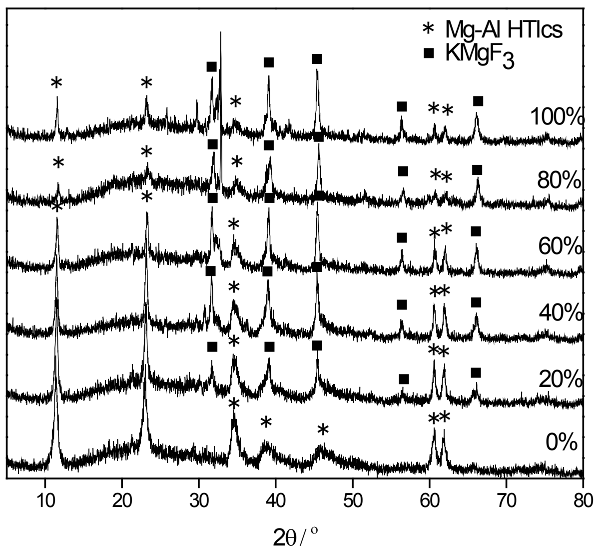

Fig. S5 XRD patterns of KF/Mg-Al HTlcs with different loading amount of KF.

Table S1 Nitrogen physisorption data of HTlcs

Entry	Catalyst	Surface Area (m^2 g^{-1})	Pore Volume (cm^3 g^{-1})	Average pore width (Å)
1	Mg-Al HTlcs	140	0.16	45
2	Ni -Al HTlcs	272	0.55	73
3	Co-Al HTlcs	166	0.51	180
4	Cu-Al HTlcs	59	0.17	120
5	Mg-Fe HTlcs	164	0.85	278
6	Ni-Fe HTlcs	182	0.59	181
7	Cu-Fe HTlcs	139	0.47	122
8	Zn-Cr HTlcs	100	0.36	107
9	Co-Cr HTlcs	216	0.33	52